Carbon 159 (2020) 598–610

Contents lists available at ScienceDirect

Carbon

journal homepage: www.elsevier.com/locate/carbon

Keratinocytes are capable of selectively sensing low amounts of graphene-based materials: Implications for cutaneous applications

Laura Fusco [a], Marco Pelin [b], Sourav Mukherjee [c], Sandeep Keshavan [c], Silvio Sosa [b], Cristina Martín [d], Viviana González [d], Ester Vázquez [d, e], Maurizio Prato [a, f, g], Bengt Fadeel [c, *], Aurelia Tubaro [b, **]

[a] Department of Chemical and Pharmaceutical Sciences, University of Trieste, 34127, Trieste, Italy
[b] Department of Life Sciences, University of Trieste, 34127, Trieste, Italy
[c] Institute of Environmental Medicine, Karolinska Institutet, 171 77, Stockholm, Sweden
[d] Department of Organic Chemistry, Instituto Regional de Investigación Científica Aplicada (IRICA), Universidad de Castilla-La Mancha, 13071, Ciudad Real, Spain
[e] Department of Organic Chemistry, Facultad de Ciencias y Tecnologías Químicas, Universidad de Castilla-La Mancha, 13071, Ciudad Real, Spain
[f] Bionanotechnology Laboratory, CIC BiomaGUNE, 20009, San Sebastián, Spain
[g] Ikerbasque, Basque Foundation for Science, 48013, Bilbao, Spain

ARTICLE INFO

Article history:
Received 21 September 2019
Received in revised form
21 December 2019
Accepted 23 December 2019
Available online 24 December 2019

ABSTRACT

Skin provides the first interface between body and environment, representing one of the most feasible exposure routes to graphene-based materials (GBMs). However, interactions of GBMs with the skin are poorly understood. In particular, low-concentration effects have not been investigated. Here we explored the ability of endotoxin-free, few-layer graphene (FLG) and dehydrated graphene oxide (d-GO) to initiate an inflammatory response at the cutaneous level by using human HaCaT keratinocytes. HaCaT cell exposure to low concentrations (0.01–1.0 μg/mL) of FLG or d-GO did not affect cell viability. FLG triggered the secretion of pro-inflammatory tumor necrosis factor-α (TNF-α), interleukin (IL)-1α, and IL-6, while d-GO, and to a lesser extent FLG, prompted IL-8 (CXCL8) production. However, conditioned medium from HaCaT cells exposed to FLG or d-GO had no effect on THP-1 monocyte activation. Moreover, co-culture experiments did not show any effect of FLG- or d-GO-treated HaCaT cells on THP-1 cell migration. These results suggest that while GBMs are able to initiate an inflammatory response in keratinocytes, this does not necessarily lead to activation of monocytes. The present findings are relevant for potential dermal exposures to GBMs in occupational settings as well as the use of GBMs for cutaneous applications such as in wearable sensors.

1. Introduction

Graphene and its derivatives, e.g., few-layer graphene (FLG), graphene oxide (GO), reduced graphene oxide (rGO), and graphene nanoplatelets (GNPs), collectively known as graphene-based materials (GBMs), have gained considerable attention in recent years, due to their extraordinary physico-chemical properties [1–3]. GBMs are currently being explored in many fields, including in biomedicine [4–6]. In particular, the prospect of wearable or implantable bioelectronics using two dimensional (2D) materials has gained traction [7,8], and the unique characteristics of graphene, such as flexibility, transparency, and ease of functionalization, may enable superior device performance [8]. However, before their introduction into the market, the safety of GBMs-enabled products and devices for humans and the environment must be addressed [9]. To date, the potential toxicity of GBMs has been studied mainly in relation to inhalation, intravenous, and oral exposures [9,10], while there is a paucity of data concerning their effects at the skin level. Nevertheless, skin contact is one of the major exposure routes for GBMs, especially during their production as dry powders as well as their potential use for biomedical applications, including as soft bioelectronics [9]. Recent studies have shown that GBMs may elicit pro-inflammatory and/or cytotoxic

* Corresponding author.
** Corresponding author.
E-mail addresses: bengt.fadeel@ki.se (B. Fadeel), tubaro@units.it (A. Tubaro).

https://doi.org/10.1016/j.carbon.2019.12.064

effects on innate immune cells, including macrophages [11–15]. However, only a few *in vitro* studies have attempted to assess the biocompatibility of GBMs at the cutaneous level using skin fibroblasts [16], or keratinocytes [17–19]. The latter studies highlighted the ability of GO and FLG to induce significant cytotoxic effects, albeit at high concentrations. For instance, we recently demonstrated that GO and FLG induce significant cytotoxic effects on human HaCaT keratinocytes at concentrations higher than 1 and 30 μg/mL, respectively, after exposure of the cells for 72 h, with the effects being more pronounced at 100 μg/mL [17]. The effects on HaCaT cells were subsequently found to be due to a sustained mitochondrial depolarization and production of reactive oxygen species (ROS) [18]. It is important to note that keratinocytes are immune-competent sentinels of the skin with the ability to 'sense' pathogens or other danger signals *via* so-called pattern recognition receptors with the release of pro-inflammatory mediators [20,21]. In addition, various specialized immune cells, including subsets of dendritic cells (DCs) and T cells, are also present in the skin [20]. Hence, understanding whether GBMs exert pro- or anti-inflammatory effects on keratinocytes or other immune-competent cells present in the skin is of key importance. The present study was designed with the aim to explore effects of low concentrations of GBMs at the cutaneous level using an *in vitro* model. To this end, we deployed human HaCaT keratinocytes and human THP-1 monocytes. Two carefully characterized FLG and GO materials were evaluated following direct exposure of HaCaT cells as well as indirect exposure of THP-1 cells cultured in conditioned medium of FLG- or GO-exposed HaCaT cells. Care was taken to ensure that the GBMs were endotoxin-free as this may otherwise confound the results. Overall, the present study has disclosed that human skin cells can sense sub-cytotoxic concentrations of GBMs.

2. Experimental section

2.1. GBM characterization

The thermogravimetric analysis (TGA) were performed with a TGA Q50 (TA Instruments) at 10 °C/min under a N_2 atmosphere, from 100 to 800 °C, preceded by an isotherm at 100 °C for 20 min in order to remove possible traces of moisture. Raman characterization was carried out using an InVia Renishaw microspectrometer. The Raman sample was prepared from a stable dispersion of materials by drop-casting over silicon oxide surface, and left to evaporate in ambient conditions. Raman spectra were acquired with the 532 nm laser, at an incident power of 1% for 10 s of exposure time and using a 100 × objective. To perform transmission electron microscopy (TEM) analysis, a stable material dispersion was drop-cast on a carbon-coated microscopy grid, and dried under vacuum. The sample was studied by high-resolution TEM using a JEOL 2100 at an accelerating voltage of 100 kV. Elemental analysis and X-ray fluorescence of graphene powder were performed using an elemental analyzer (LECO CHNS-932, model no. 601-800-500) and a Bruker-S2 PicoFox TXRF spectrometer, respectively.

2.2. Preparation of FLG

Aqueous dispersions were obtained through a ball-milling procedure on a dry basis and under an air atmosphere, as described previously [22,23]. Briefly, 30 mg of graphite/melamine mixture (1:3) was ball-milled at 100 rpm for 30 min. The resulting solid mixture was transferred to an Erlenmeyer flask using 20 mL of Milli-Q water and ultrasonication led to a dark suspension. Melamine was removed by washing the dispersion by dialysis with hot water. The obtained suspension was left to settle for five days and the unreacted graphite was removed. The liquid fraction with stable sheets in suspension was carefully extracted to provide FLG. Afterwards, the aqueous dispersion was lyophilized and a powder was obtained. Characterization of the powder was conducted by means of TGA, total reflection X-ray fluorescence (TRXF), Raman spectroscopy, TEM, and elemental analysis (EA).

2.3. Preparation of GO

GO was obtained from Graphenea group (San Sebastián, Spain). Characterization of the powder was conducted by means of TGA, Raman spectroscopy, TEM, and EA, as described previously by us [17].

2.4. Endotoxin-free FLG

Endotoxin-free FLG was obtained by heat treatment of the FLG powder. The thermal treatment was performed by using a TGA Q50 (TA Instruments) under N_2 conditions, and it consisted of three different stages: a first heating ramp at 10 °C/min up to 129 °C, followed by an isothermal segment for 60 min, and finally a cooling ramp (2 °C/min until 25 °C). All the materials used to manipulate the sample were previously rinsed with isopropanol and endotoxin-free Eppendorf tubes were used to store the treated FLG. Subsequently, the material was re-characterized by TGA and Raman spectroscopy.

2.5. Endotoxin-free GO

The endotoxin removal was performed by heat treatment of samples at 200 °C for 1 h in a protective Ar atmosphere. Subsequently, the material was re-characterized to evaluate any physicochemical alterations.

2.6. Endotoxin content

The tumor necrosis factor (TNF-α) expression test (TET) was used for assessment of endotoxin content [24]. Briefly, primary human monocyte-derived macrophages (HMDMs) were obtained from human monocytes isolated from healthy donors by using a Lymphoprep™ density gradient (Axis-Shield, Oslo, Norway) [25]. The samples were anonymized and results cannot be traced back by the researchers to the individual donors; therefore, no specific ethical permission is needed. Cells were exposed to GBMs in culture medium in the presence or absence of 10 μM polymyxin B (Sigma-Aldrich). LPS (100 ng/mL) (Sigma-Aldrich) was included as a positive control. Cell supernatants were then collected and the production of TNF-α was monitored by ELISA (Mabtech, Nacka Strand, Sweden).

2.7. Cell culture

HaCaT cells were cultured in Dulbecco's Modified Eagle's medium (DMEM) high glucose, supplemented with 10% fetal bovine serum (FBS), 1.0×10^{-2} M L-glutamine, 1.0×10^{-4} g/mL penicillin and 1.0×10^{-4} g/mL streptomycin at 37 °C in a humidified 95% air/5% CO_2 atmosphere. Cell passage was performed 2 days post-confluence, once a week. All the experiments were performed between passage 44 and 70. For GBM exposures, cells were incubated with FLG or d-GO under non-confluent conditions. THP-1 cells were cultured in RPMI-1640 supplemented with 10% FBS, 1.0×10^{-2} M L-glutamine, 1.0×10^{-4} g/mL penicillin and 1.0×10^{-4} g/mL streptomycin at 37 °C under a humidified 95% air/5% CO_2 atmosphere. The experiments were performed between passage 7 and 20. As positive controls for monocyte differentiation (see Supporting Information), undifferentiated THP-1 monocytes were differentiated

using previously described protocols [26] into: *i*) macrophages by treatment with 10^{-7} M phorbol-12-myristate-13-acetate (PMA) for 72 h; *ii*) immature dendritic cells (iDCs) by exposure to 100 ng/mL interleukin (IL)-4 and granulocyte-macrophage colony-stimulating factor (GM-CSF) for 120 h; or *iii*) mature dendritic cells (mDCs) by exposure to 200 ng/mL IL-4, 100 ng/mL GM-CSF, 10 ng/mL TNF-α, and 200 ng/mL ionomycin in serum-free medium for 48 h.

2.8. Cell viability

The effects of GBMs on cell viability were evaluated by the 2-(2-methoxy-4-nitrophenyl)-3-(4-nitrophenyl)-5-(2,4-disulfophenyl)-2H-tetrazolium (WST-8) reduction assay. After GBMs exposure, cells were washed three times with PBS (200 μL/well) and incubated for 4 h with fresh medium (100 μL/well) containing 10 μL of WST-8 reagent. Absorbance was subsequently determined at 450 nm by an Automated Microplate Reader EL 311s (Bio-Tek Instruments, Winooski, VT). Data are reported as % cell viability in cells exposed to GBMs with respect to untreated control cells. Cell viability of HMDMs was determined by using the Alamar Blue assay, as previously described [27].

2.9. Cellular uptake

To evaluate cellular uptake, HaCaT cells were exposed to FLG or d-GO at a concentration of 10 μg/mL. After exposure for 4 h or 24 h, cells were fixed in 2.5% glutaraldehyde in 0.1 M phosphate buffer, pH 7.4 at room temperature for 30 min and further fixed overnight in the refrigerator. Samples were then rinsed in 0.1 M phosphate buffer and centrifuged. The pellets were post-fixed in 2% osmium tetroxide in 0.1 M phosphate buffer, pH 7.4 at 4 °C for 2 h, dehydrated in ethanol followed by acetone and embedded in LX-112. Ultrathin sections (approx. 50–60 nm) were cut by using a Leica ultracut UCT/Leica EM UC 6. Sections were contrasted with uranyl acetate followed by lead citrate and examined using a Tecnai 12 Spirit Bio TWIN transmission electron microscope (FEI Company) at 100 kV/Hitachi HT 7700. Digital images were taken using a Veleta camera (Olympus).

2.10. Cytokine analysis

The effects of sub-cytotoxic concentrations of GBMs on the release of selected inflammatory cytokines by HaCaT cells were evaluated using the Procarta Plex Mix & Match kit (eBioscience, Milan, Italy), based on Luminex® technology, as previously described [27]. Briefly, HaCaT cells were seeded overnight at a density of 3×10^4 cells/well in 24-well plates and exposed to GBMs. Control media were collected from cells cultured in GBM-free medium. As a positive control, cells were exposed to 10 μg/mL LPS for 24 h. Thereafter, the supernatants were collected and the following panel of mediators was quantified: IL-1α, IL-6, IL-8, IL-10, interferon (IFN)-α, macrophage inflammatory protein (MIP)-1β, TNF-α, and GM-CSF. THP-1 cells were seeded at a density of 2×10^5 cells/well in 24-well plates and exposed for 24 h to HaCaT-conditioned media collected after recovery exposures ("4h + 20h" and "4h + 68h") or control HaCaT-conditioned media, followed by 24 h culture in fresh media. Subsequently, the supernatants were collected and kept at −80 °C until analysis. The following inflammatory mediators, released by THP-1 cells, were quantified by Luminex® system using the Bio Plex Pro™ human cytokine strandard 27-plex kit (BioRad; Solna, Sweden) covering the following biomarkers: IL-1 receptor antagonist (IL-1Ra), IL-1β, IL-2, IL-4, IL-5, IL-6, IL-7, IL-8, IL-9, IL-10, IL-12, IL-13, IL-15, IL-17, Eotaxin, basic fibroblast growth factor (FGF basic), granulocyte-colony stimulating factor (G-CSF), GM-CSF, IFN-γ, interferon gamma-induced protein 10 (IP-10), monocyte chemoattractant protein (MCP)-1, platelet-derived growth factor (PDGF)-BB, regulated on activation normal T cell expressed and secreted (RANTES), TNF-α, VEGF, MIP-1α, and MIP-1β. As a positive control, cells were exposed to 0.1 μg/mL LPS for 24 h.

2.11. Flow cytometry

The expression of specific differentiation markers (CD14, CD54, CD86, CD11b, and HLA-DR) on the cell surface of THP-1 cells was evaluated by flow cytometry. Briefly, cells were labeled with mouse monoclonal antibodies (mAbs) conjugated with: Alexa Fluor 700 specific for CD14, PE-Cy™ 5 specific for CD54, fluorescein isothiocyanate (FITC) specific for CD86, and with phycoerythrin (PE) specific for HLA-DR and CD11b, according to the manufacturer's instructions (BD Pharmingen, San Diego, CA). THP-1 cells (2×10^5 cells/well) were seeded in 6-well plates and exposed for 48 or 120 h to HaCaT-conditioned media collected after recovery exposures ("4h + 20h" and "4h + 68h") or control HaCaT-conditioned media. Subsequently, cells were collected, washed with PBS and fixed with 1 mL of 4% paraformaldehyde for 30 min at 4 °C. Cells were then washed with 1 mL of PBS and the pellet was suspended in 50 μL of FACS buffer (0.5% bovine serum albumin, and 0.01% sodium azide in PBS) in the presence of 4% Fc receptor blocking reagent (Miltenyi Biotec, Auburn, CA) in which 3 μL of each antibody were added. Cells were incubated with antibodies at 4 °C for 30 min and subsequently washed with 300 μL of FACS buffer. The pellet was then suspended in 300 μL of FACS buffer. Fluorescence was measured with a BD LSRFortessa™ Cell Analyzer (BD Biosciences; Stockholm, Sweden). Ten thousand cells were counted and the data were analyzed by using the BD FACSDiva Software (BD Biosciences). To ensure that the fluorescence signal detected was due to the antibodies of interest, a process of compensation was applied for each fluorochrome to remove the signal falling within the detector of another fluorochrome by using Compbeads® (BD Biosciences).

2.12. Chemotaxis assay

THP-1 migration was evaluated in 24-well plates in a co-culture system with HaCaT cells using Transwell® inserts with 8 μm pores (Corning, Milan, Italy). HaCaT cells (3×10^4 cells/well) were seeded in 24-well plates (lower compartment) and exposed to GBMs (0.1 and 1.0 μg/mL) under the recovery conditions "4h + 20h" and "4h + 68h". At the end of GBMs exposure, THP-1 cells were incubated with 10^{-4} M 1,1′-dioctadecyl-3,3,3′,3′-tetramethylindocarbocyanine perchlorate (DiL) at 37 °C for 20 min. After washing, 2×10^5 THP-1 cells were added in each Transwell® insert (upper compartment) and co-cultured with HaCaT cells, previously seeded in the lower compartment, for 4 h at 37 °C. MIP-3α (1.25×10^{-12} M) was included as a positive control, whereas the negative control was represented by HaCaT cells not exposed to GBMs. After 4 h, fluorescence was read in the lower compartment ("migrated cells") and in the inserts (upper compartment) after two washes ("migrating cells") using a Fluorocount Microplate Fluorometer (Packard; Milan, Italy). The data are presented as % increase of chemotaxis of migrated and migrating cells with respect to the untreated control cells.

2.13. Statistical analysis

Results shown are the mean values ± standard error (SE) of at least three independent experiments performed in triplicate. The inflammatory mediator data for HaCaT cells were analyzed by one-way ANOVA and Tukey's Multiple Comparison Test

(PrismGraphPad, Inc.; San Diego, CA). THP-1 cell differentiation and migration data were analyzed by one-way ANOVA and Bonferroni post-test (PrismGraphPad, Inc.; San Diego, CA). Differences were considered significant at $p < 0.05$. Hierarchical cluster analysis of the cytokine data and the generation of heatmaps was performed using R [27].

3. Results

3.1. Material characterization and endotoxin removal

The materials initially considered for this study were prepared by ball-milling of graphite, as previously described (FLG) [18,22], or were provided by a commercial supplier (GO). Both materials were fully characterized with respect to their physico-chemical properties (Supplementary Fig. S1) and tested for endotoxin content as detailed in previous publications [24,28]. The TET assay, based on TNF-α expression in primary human macrophages exposed to sub-cytotoxic concentrations of the test material, with or without the LPS inhibitor, polymyxin B, demonstrated the presence of endotoxin in both materials (GO > FLG). Therefore, FLG and GO were heat-treated to remove LPS. After heat treatment, both materials were non-cytotoxic for macrophages, and endotoxin-free (Supplementary Fig. S2).

After endotoxin removal, FLG and GO were re-characterized by TGA and Raman spectroscopy to define any structural alterations resulting from the heat treatment (Fig. 1). In the case of FLG, TGA did not show any changes before and after thermal treatment, resulting in a 4 wt% of loss at 600 °C (Fig. 1B). This value is in agreement with the oxygen percentage obtained from the EA of FLG (Supplementary Fig. S1). In addition, Raman signals remained almost unchanged (Fig. 1A). The average Raman spectra of FLG, before and after thermal treatment, showed the two most intense peaks of graphene, the G band and the 2D peak, which appear at around ~1576 cm^{-1} and ~2700 cm^{-1}, respectively. The average I (2D)/I(G) ratios for FLG are 0.48 and 0.42 before and after the thermal treatment, respectively, proving the samples to be few-layer graphene, usually assigned for I (2D)/I(G) < 1 [29,30]. In addition, the full-width at half maximum (FWHM) of the 2D band was 67.3 and 65.4 before and after the thermal treatment, respectively. When defects occur in graphene, a peak appears at around 1345 cm^{-1} (D band). In the present case, the average spectra of FLG showed I(D)/I(G) ratios of about 0.4 and 0.36 before and after thermal treatment, respectively, corroborating the low level of defects attributed to the edges of the micrometer flakes [31]. Overall, TGA and Raman spectroscopy confirmed that the physico-chemical properties of FLG were unaffected by endotoxin removal. In contrast, TGA of GO showed a clear difference before and after the thermal treatment, resulting in a 44.81 wt% of loss at 600 °C for GO and only 28.27 wt% of loss at the same temperature for GO after the thermal treatment (Fig. 1D). The mass loss below 170 °C is normally attributed to the removal of absorbed water, while the loss above 170 °C corresponds to the loss of the oxygen functional groups [32,33]. Accordingly, the TGA results of GO after thermal treatment can be ascribed not only to the evaporation of water, but also to the partial loss of labile oxygen groups during endotoxin

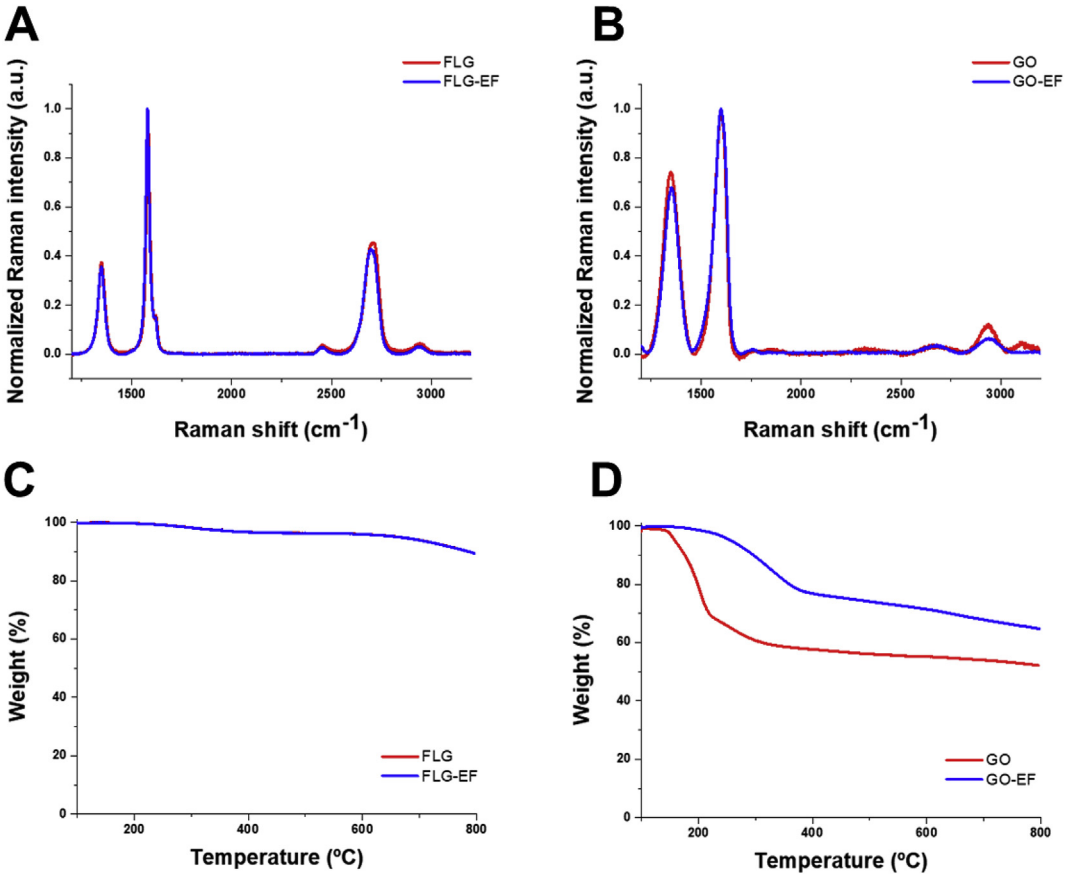

Fig. 1. Characterization of FLG and GO before and after ("FLG-EF" and "GO-EF" samples) thermal treatment for endotoxin removal (Supp. Fig. S2). (A) Normalized average Raman spectra (at least 15 different spectra from different sample locations) of FLG samples; (B) TGA curves of FLG samples; (C) normalized average Raman spectra (at least 15 different spectra from different sample locations) of GO samples; (D) TGA curves of GO samples.

elimination. This is in agreement with a previous study showing partial reduction of GO at low temperatures [34]. In addition, Raman signals varied slightly. Hence, the average Raman spectra of the GO samples before and after treatment (Fig. 1C) showed the two most intense peaks of GO, the G band and the D peak, which appear at around ~1600 cm-1 and ~1350 cm-1, respectively. The average spectra of GO samples showed I(D)/I(G) ratios about 0.76 and 0.68 before and after the thermal treatment, respectively, corroborating the high level of defects which are present in these flakes. Thus, TGA and Raman spectroscopy showed that the properties of GO were mildly affected by endotoxin removal. However, the most probable event occurring during the thermal treatment of GO is the loss of water to form a double bond, thus restoring part of the p-extended system of graphene. Since, strictly speaking, this is not a reduction process, we decided to designate the heated GO as dehydrated GO (d-GO).

3.2. Experimental design and concentration selection

We previously studied the impact of FLG and GO on HaCaT cells at concentrations ranging from 1 to 100 μg/mL. No significant cytotoxic effects were noted at 24 h, but a concentration-dependent cytotoxicity was observed after 72 h of exposure, and GO was more cytotoxic than FLG [17]. We also performed long-term experiments in which the cells were maintained for 14 days in the presence of 0.1 μg/mL of GBMs, but we noted only slight effects on cell viability [17]. Here we decided to explore the effects, if any, of low concentrations of endotoxin-free FLG or d-GO, and we elected to expose cells to 0.01, 0.1, and 1.0 μg/mL for 4, 24, and 72 h (continuous exposures) or, alternatively, to the same concentrations of endotoxin-free FLG or d-GO for 4 h, followed by three washes with PBS and further incubation for an additional 20 or 68 h in fresh medium without GBMs added, i.e., “4h + 20h” (24 h) and “4h + 68h” (72 h) recovery exposures, respectively. The reason for choosing to study cells after recovery was to mimic, to the extent that this is possible, the occupational exposure experienced during one half (4 h) of a work shift (exposure followed by recovery). After each exposure, cell viability and the release of a panel of inflammatory mediators from HaCaT cells were evaluated. The experimental conditions showing the highest release of inflammatory mediators, namely “4h + 20h” and “4h + 68h” recovery exposures at GBMs concentrations of 0.1 and 1.0 μg/mL (see below) were chosen to investigate whether HaCaT cells exposed to endotoxin-free GBMs were able to modulate THP-1 monocyte chemotaxis at 4 h, monocyte secretion of inflammatory mediator release at 24 h, and monocyte differentiation up to 120 h. To evaluate monocyte responses, THP-1 cells were exposed to conditioned medium obtained as follows: HaCaT cells were exposed to endotoxin-free FLG or d-GO (0.1 and 1.0 μg/mL) for 4 h, washed three times with PBS, and incubated for 20 and 68 h in fresh medium (”4h + 20h” and “4h + 68h”), respectively. Control media samples were collected from HaCaT cells cultured in FLG- and d-GO-free medium for the same length of time.

We are not aware of any measurements of the actual dermal exposure to GBMs in the workplace or in any other exposure setting. However, based on surveys of workplaces where carbon nanotubes (CNTs) are manufactured, Palmer et al. [35] estimated that the potential dermal exposures to CNTs could be in the range of 0.5–14.5 μg/cm^2. Moreover, due to the use of personal protective equipment, the authors suggested that it is likely that only a small fraction of the deposited concentration contacts the skin, and concluded that low-concentration studies are the most relevant ones [35]. Taking the current cell culture model into consideration, we find that the concentrations of 1.0, 0.1, and 0.01 μg/mL correspond to approximately 0.5, 0.05 and 0.005 μg/cm^2, lower than the potential dermal exposure range estimated for CNTs. In other words, the concentrations that we have applied here (see the following sections) may be considered as relevant for the occupational setting.

3.3. Low-concentration effects of GBMs on keratinocytes

The effect of FLG and d-GO on HaCaT cells following continuous exposure for 4, 24, and 72 h, or exposure for 4 h with recovery for 20 and 68 h was determined by using the WST-8 assay, showing no reduction of cell viability for all the experimental conditions (Fig. 2A and B). The effects of endotoxin-free FLG and d-GO on the release of selected cytokines by HaCaT keratinocytes were evaluated after continuous cells exposure (4, 24, and 72 h) to sub-cytotoxic concentrations of FLG or d-GO (0.01, 0.1, and 1.0 μg/mL) and after cells exposure for 4 h followed by incubation in fresh GBMs-free culture medium (”4h + 20h” and “4h + 68h” recovery exposure). Remarkably, IL-1α secretion was significantly upregulated following recovery exposure (”4h + 20h” and “4h + 68h”) to FLG and this effect was noted already at the lowest concentration (0.01 μg/mL). d-GO also increased IL-1α secretion, in particular after recovery exposure (”4h + 68h”) though this effect was not as pronounced as for FLG (Fig. 3A). Furthermore, FLG, but not d-GO, triggered the secretion of IL-6, and this was most pronounced after recovery exposure and was noted already at the lowest concentration (0.01 μg/mL) (Fig. 3B). In contrast, d-GO exerted the strongest effect on IL-8 following recovery exposure (”4h + 20h” and “4h + 68h”) and the effect was, again, noted already at the lowest concentration, while FLG only elicited IL-8 secretion at the highest concentration (1.0 μg/mL) (Fig. 3C). FLG also triggered the secretion of TNF-α at the highest concentration, while d-GO had no effect (Fig. 3D). Finally, both FLG and d-GO induced a slight, but significant, increase of GM-CSF secretion (Supplementary Fig. S3), though this was not as pronounced as that induced by LPS. In contrast, the release of inflammatory IFN-α, anti-inflammatory IL-10, and MIP-1β was not detected following continuous exposure to GBMs or during recovery conditions (data not shown). To further analyze the cytokine secretion results, hierarchical cluster analysis was performed to draw association dendrograms between exposure conditions and cytokines, as reported previously [27]. Interestingly, our analysis showed distinct patterns of cytokine production and associations with the different exposure conditions. Thus, two major clusters, the first one comprising of the continuous exposure samples and the second one consisting of the recovery samples, were identified (Fig. 4, refer to dendrogram to the left of the heatmap). The LPS treated samples segregated with the second cluster. IL-8 (CXCL8) showed a distinct pattern from the other cytokines (Fig. 4, refer to the dendrogram at the top of the heatmap). Overall, the GBMs induced the highest production of inflammatory cytokines (IL-1α, IL-6, IL-8, TNF-α, and GM-CSF) in HaCaT cells after 4 h exposure to 0.1 and 1.0 μg/mL followed by 20 h or 68 h recovery in fresh medium (”4h + 20h” and “4h + 68h”). For this reason, these conditions were chosen for the subsequent experiments using THP-1 cells as a model of monocytes [27].

We previously reported that GO and FLG are internalized by HaCaT cells as evidenced by Raman spectroscopy [18]. Here, we performed TEM analysis to verify cellular uptake of these materials. To this end, HaCaT cells were incubated with 10 μg/mL of d-GO or FLG and samples were collected for TEM analysis. We used a higher dose of d-GO or FLG for this assay as compared to other assays reported in the current study to ensure the detection of the materials in cells by TEM. As shown in Fig. 5, both d-GO and FLG were taken up by HaCaT cells in the absence of ultrastructural signs of toxicity.

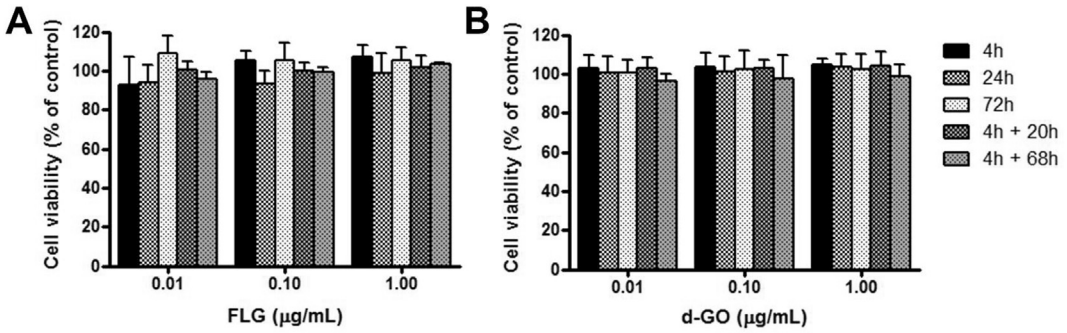

Fig. 2. FLG and d-GO are non-cytotoxic to keratinocytes at low concentrations. HaCaT cells were exposed to endotoxin-free FLG (A) or d-GO (B) for 4, 24 and 72 h (continuous exposures) or, alternatively, for 4 h followed by a further 20 or 68 h in fresh cell medium free of GBMs ("4h + 20h" and "4h + 68h" recovery exposures, respectively). Cell viability was evaluated by the WST-8 assay. Data are reported as % cell viability in cells exposed to FLG or d-GO in comparison to untreated control and are mean values ± S.E. of three independent experiments.

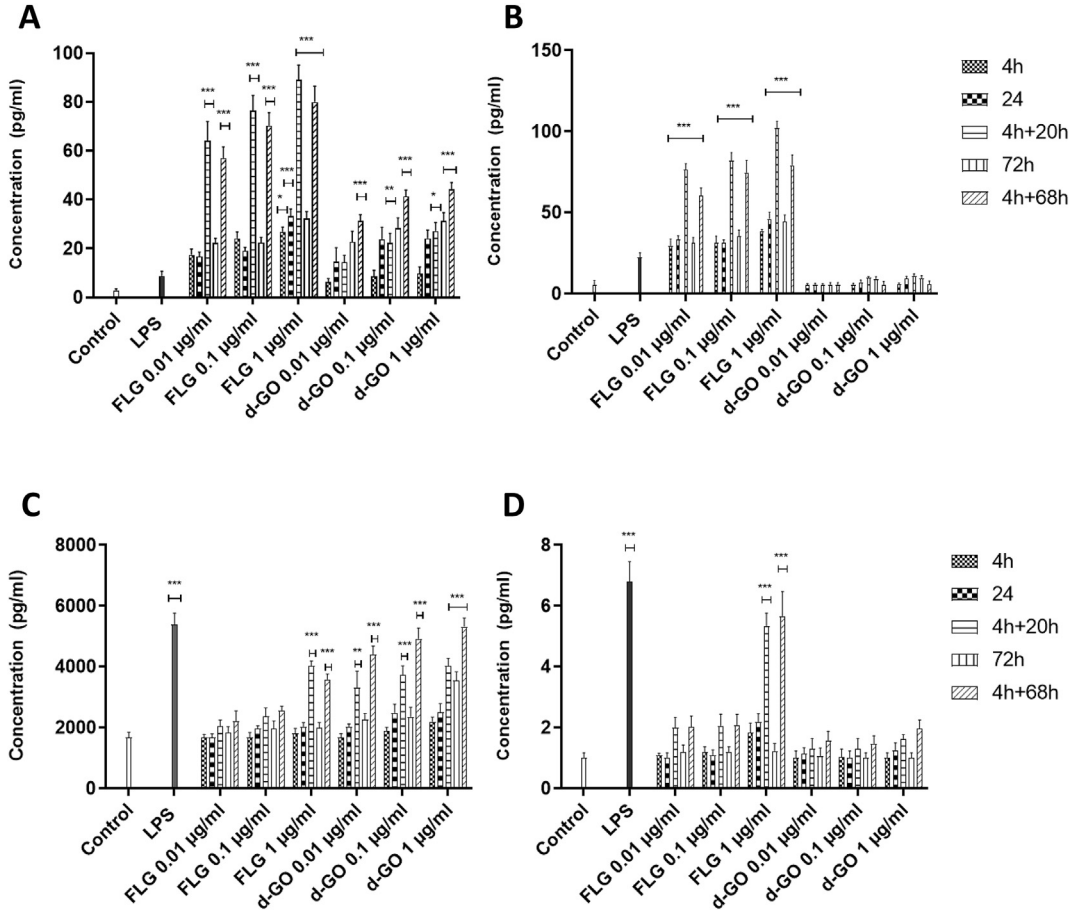

Fig. 3. FLG and d-GO elicit cytokine responses in keratinocytes at low concentrations. Multiplex profiling of the inflammatory mediators, (A) IL-1α, (B) IL-6, (C) IL-8, and (D) TNF-α released by HaCaT cells exposed to endotoxin-free FLG or GO continuously (4, 24 and 72 h) and following a 4 h exposure and followed by recovery (4h + 20h and 4h + 68h). LPS (10 μg/mL) was included as a positive control. Results are presented as mean values ± S.E. of three independent experiments. *p value ᶜ0.05, **pᶜ0.01, ***pᶜ0.001 (One-way ANOVA and Tukey's Multiple Comparison Test).

3.4. Monocyte secretion of cytokines/chemokines

Next, we tested whether conditioned media from exposed HaCaT cells had any effect on THP-1 cells. To this end, conditioned media collected from HaCaT cells under recovery conditions (cells exposed to 0.1 and 1.0 μg/mL endotoxin-free FLG or d-GO for 4 h followed by culture in GBMs-free medium for 20 h or 68 h, i.e., "4h + 20h" and "4h + 68h" recovery exposure) were evaluated for their ability to induce the release of cytokines, chemokines and growth factors from THP-1 cells. THP-1 cells were thus exposed for 24 h to conditioned medium that was subsequently replaced with fresh medium, maintaining the cells in culture for a further 24 h. The conditioned medium was removed after 24 h to avoid any interference of inflammatory mediators previously released by the HaCaT cells. As positive control, THP-1 cells were exposed to 0.1 μg/mL LPS for 24 h whereas the negative control is represented by

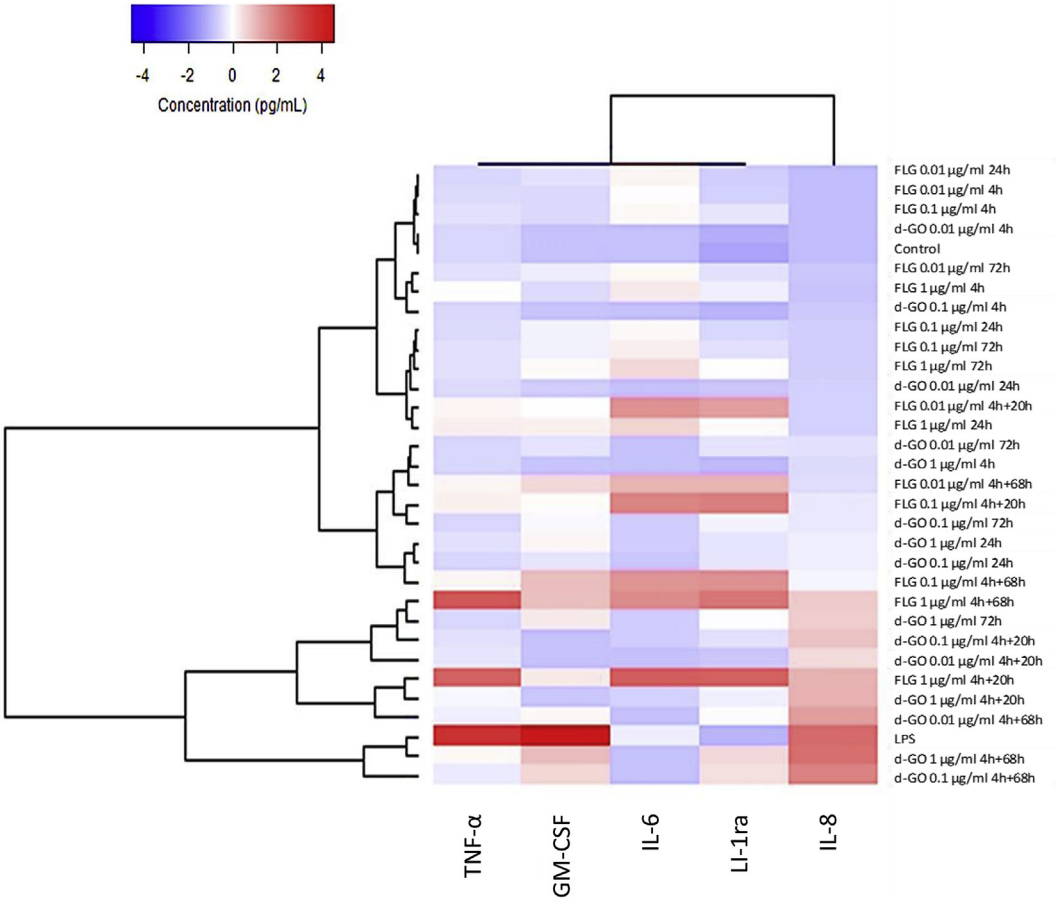

Fig. 4. Cytokine responses after continuous exposure or recovery conditions. Hierarchical cluster analysis of inflammatory mediators released by HaCaT cells exposed to FLG or d-GO continuously (4, 24 and 72 h) or for 4 h exposure followed by recovery (4h + 20h and 4h + 68h). As positive control, cells were exposed to 10 µg/mL LPS for 24 h. Each branch in the dendrograms shows the similarity between samples; the shorter the branch, the more similar the samples. Association clusters for exposures and cytokines are represented by dendrograms at the left and at the top of the heat map, respectively.

THP-1 cells exposed to conditioned media collected from HaCaT cells not exposed to FLG or d-GO. The samples were analyzed by using the Bio Plex Pro™ 27-plex human cytokine assay, and results were subjected to hierarchical cluster analysis as described above for HaCaT cells. Overall, the release of cytokines, chemokines and growth factors by THP-1 cells exposed to conditioned media was significantly lower than that induced by the positive control LPS (Fig. 6A). The results in comparison to negative control cells are reported in Fig. 5B. Conditioned media collected from HaCaT cells ("4h + 20h" and "4h + 68h") did not significantly influence cytokine release in THP-1 cells, and no obvious grouping of the different exposure conditions was noted, but the cluster analysis allowed us to draw association dendrograms between the released inflammatory mediators, suggesting two clusters, the first ranging from IFN-γ to vascular endothelial growth factor (VEGF) and the second ranging from GM-CSF to macrophage inflammatory protein (MIP)-1α (Fig. 6B).

3.5. Monocyte differentiation and cell migration

We also evaluated the effects of conditioned media collected from endotoxin-free GBMs-exposed HaCaT cells on THP-1 differentiation. To this end, THP-1 cells were exposed for 48 and 120 h to the conditioned media collected from HaCaT cells exposed to endotoxin-free FLG or d-GO (0.1 and 1.0 µg/mL) under the "4h + 20h" and "4h + 68h" recovery conditions. As a negative control, THP-1 cells were exposed to conditioned media collected from HaCaT cells not treated with FLG or d-GO. Subsequently, the expression of specific surface differentiation markers on THP-1 cells was evaluated by flow cytometry. Overall, none of the conditioned media influenced the expression of the selected differentiation markers, CD14, CD54, CD86, HLA-DR, and CD11b (Fig. 7A–H). Only a slight, yet significant, increase in the expression of HLA-DR was recorded in THP-1 cells exposed for 120 h to the "4h + 68h" conditioned medium collected from HaCaT cells exposed to the highest concentration of FLG (1.0 µg/mL) (Fig. 7D). For comparison, differentiation of THP-1 cells into macrophages or immature dendritic cells (iDCs) as well as mature dendritic cells (mDCs) using established protocols as described in the experimental methods section significantly increased the expression of the relevant differentiation markers (Supplementary Fig. S4).

Finally, to evaluate the effects of endotoxin-free FLG and d-GO treatment of HaCaT cells on THP-1 migration or chemotaxis, THP-1 cells were co-cultured for 4 h with HaCaT cells previously exposed to FLG and d-GO (0.1 and 1.0 µg/mL) under recovery conditions. THP-1 chemotaxis was then evaluated considering both the migrated and the migrating cells using a Transwell® assay [36]. As negative controls, THP-1 cells were co-cultured with HaCaT cells not exposed to FLG or d-GO. Compared to the negative controls, HaCaT cells pre-exposed to FLG (Fig. 8A) or d-GO (Fig. 8B) induced only a slight and non-significant increase of THP-1 cell migration. After "4h + 20h" recovery exposure, HaCaT cells pre-exposed to the

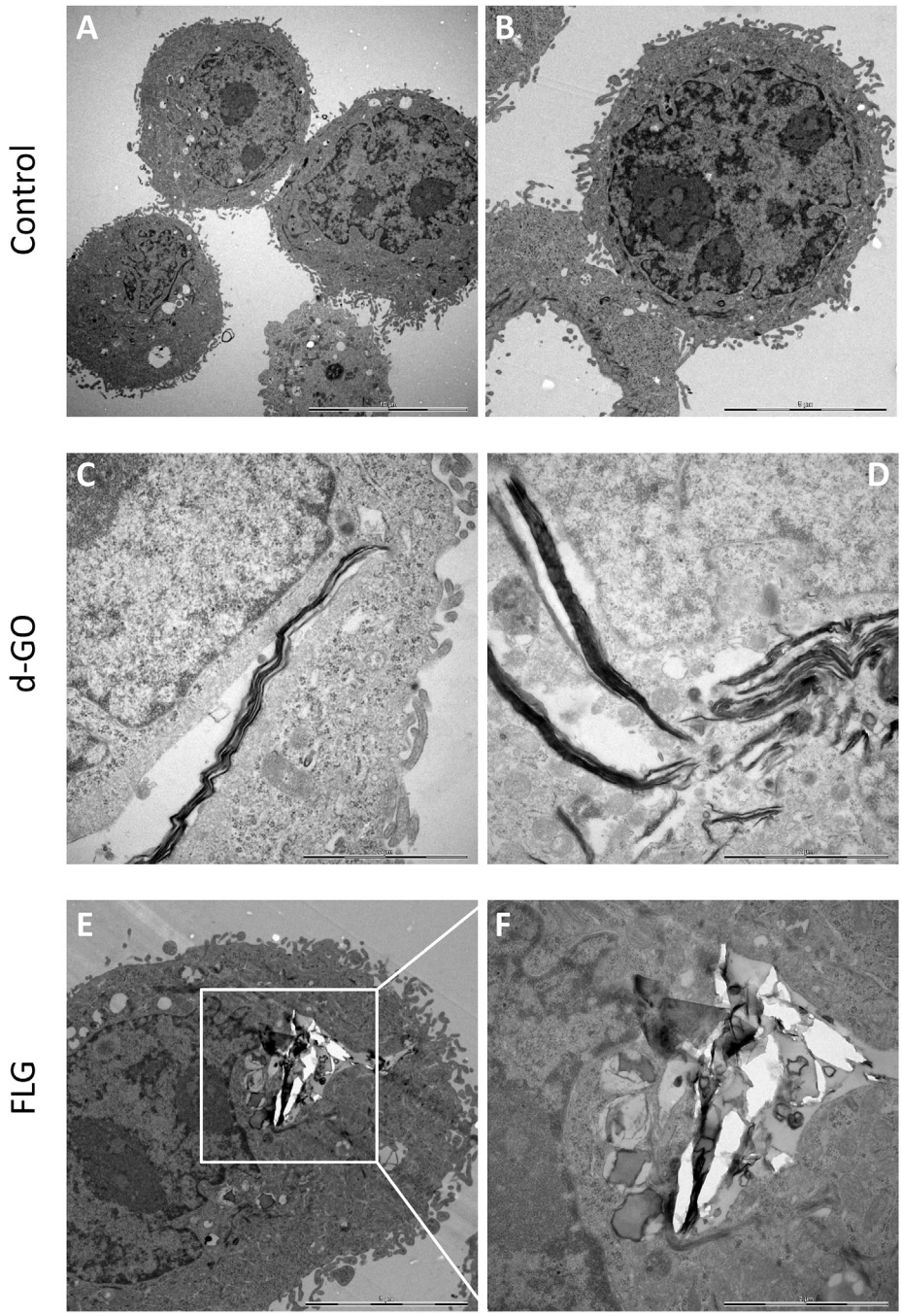

Fig. 5. FLG and d-GO internalized by HaCaT cells. Cellular interactions of d-GO and FLG were monitored by using TEM. To this end, cells were incubated with d-GO and FLG (10 μg/mL) or left untreated (control). Untreated HaCaT cells displayed normal morphological features (A, B). Uptake of d-GO was noted at 4 h (C) and 24 h (D). Internalization of FLG was observed at 4 h (E, and high magnification view of the same cell shown in panel F). Despite avid uptake of both materials, no overt signs of toxicity were observed. Scale bars: 10 μm (A), 5 μm (B), 2 μm (C, D), 5 μm (E), and 2 μm (F).

highest concentration of FLG or d-GO (1.0 μg/mL) increased the migration of THP-1 cells by 18% (3% migrated and 15% migrating cells) and 14% (4% migrated and 10% migrating cells), respectively. After "4h + 68h" recovery exposure, HaCaT cells pre-exposed to the same concentration of FLG or d-GO increased the migration of THP-1 cells by 24% (11% migrated and 13% migrating cells) and by 14% (9% migrated and 5% migrating cells), respectively. As expected, the positive control, macrophage inflammatory protein (MIP)-3α (1.25×10^{-12} M) increased the migration of THP-1 cells by 95% (22% migrated and 78% migrating cells) (Fig. 8A and B).

4. Discussion

Graphene-based devices are among those that are currently in focus in soft bioelectronics, with the aim of clinically implementing deformable devices [7,8], and applications include flexible, cutaneous biosensors, and transparent contact lenses [37–39]. Clearly, for any graphene-enabled sensors that are applied directly on the skin, biocompatibility needs to be assessed both in an acute and/or chronic setting depending on the intended use. It is important to note that nanomaterials do not necessarily have to penetrate the

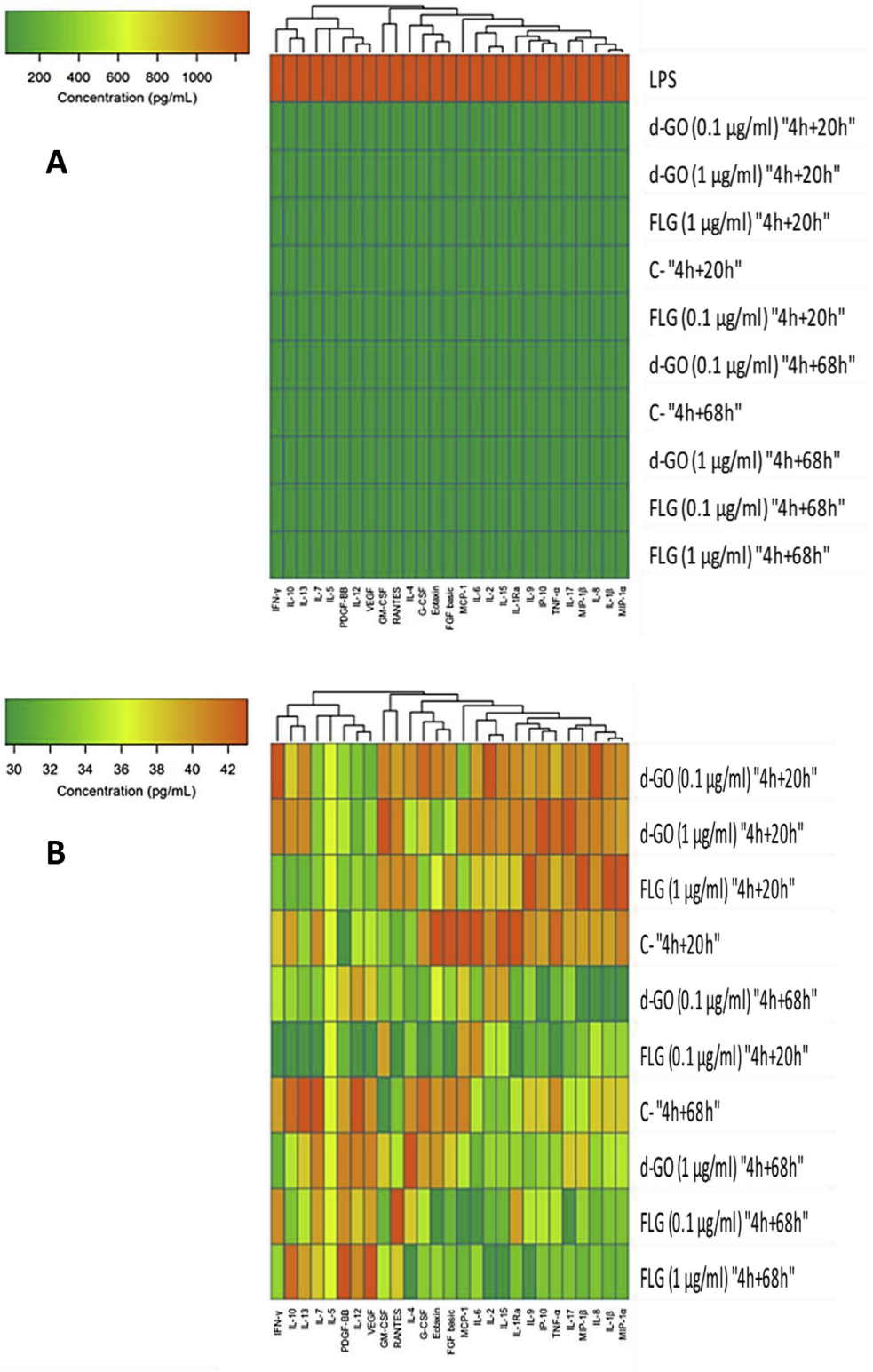

Fig. 6. Hierarchical cluster analysis of inflammatory mediators released by human monocyte-like THP-1 cells exposed to conditioned medium from HaCaT cells obtained at recovery conditions (4h + 20h, 4h + 68h, and relevant controls). As positive control, THP-1 cells were exposed to 0.1 μg/mL LPS for 24 h. Association clusters for cytokines are represented by dendrograms at the top of each heat map. (A) Heatmap of FLG and d-GO *versus* LPS (positive control). (B) Heatmap of FLG and d-GO *versus* negative control (LPS excluded from the analysis to reveal changes between the other samples).

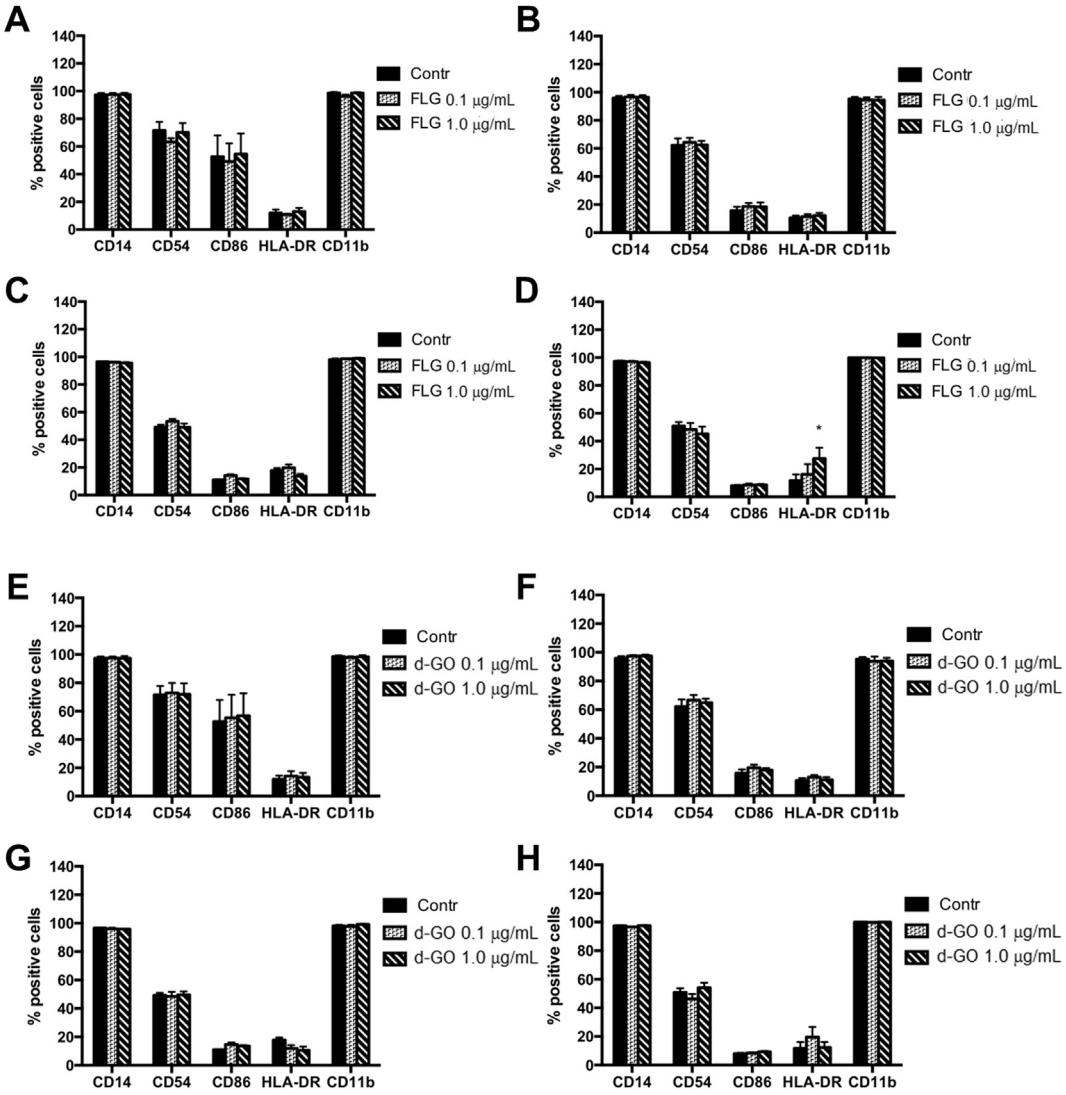

Fig. 7. No impact of conditioned medium collected from FLG- or d-GO-exposed HaCaT cells on THP-1 cells. Effects of conditioned cell culture media collected from HaCaT cells exposed to FLG (A–D) or d-GO (E–H) on monocyte differentiation were monitored by flow cytometry. THP-1 cells were exposed for 48 h to conditioned media collected from HaCaT cells exposed to FLG ("4h + 20h", panel A, and "4h + 68h", panel B) or for 120 h to the conditioned media collected from HaCaT cells exposed to FLG ("4h + 20h", panel C, and "4h + 68h", panel D). Similarly, THP-1 cells were exposed for 48 h to the conditioned media collected from HaCaT cells exposed to d-GO ("4h + 20h", panel E, and "4h + 68h", panel F) or for 120 h to the conditioned media collected from HaCaT cells exposed to d-GO ("4h + 20h", panel G, and "4h + 68h", panel H). The levels of the differentiation markers CD14, CD54, CD86, HLA-DR, and CD11b were then evaluated. The results are expressed as % of positive cells ± S.E. and are the average of three independent experiments. *, $p < 0.05$ (One-way ANOVA and Bonferroni post-test).

skin in order to exert immunomodulatory effects [40]. Previous studies have suggested that GBMs, including GO, may elicit the production of pro-inflammatory cytokines in macrophages or macrophage-like cell lines [11,12,15] and some studies have suggested that GO may signal *via* Toll-like receptors (TLRs) [41]. However, we have previously shown that CNTs, but not GO, are capable of activating TLR2 and TLR4 [36]. We also found that CNTs, but not GO, triggered NF-κB-dependent production of chemokines in primary human macrophages [36]. One confounding factor that is sometimes overlooked is the fact that nanomaterials, including GBMs, may be contaminated with endotoxin or LPS [42]. However, in the present study, we ensured that the test materials were endotoxin-free. Hence, both FLG and GO were heat-treated and were subsequently re-characterized to elucidate any structural alterations introduced by the treatment. TGA and Raman spectroscopy showed that FLG did not display any changes while the physico-chemical properties of GO were mildly affected by endotoxin removal. Since the most probable modification induced by the thermal treatment is the loss of water to form a double bond, we refer to the heated GO as dehydrated GO (d-GO). Notwithstanding, the use of endotoxin-free materials is necessary in order to avoid misleading results in biological assays [43]. The US FDA recommends to apply either high temperatures (250 °C for 45 min) or high concentrations of acids or bases to effectively remove LPS, but it is understood these conditions may also affect the properties of nanomaterials (reviewed in Ref. [44]).

Using the above referenced materials, we could show, for the first time, that low-concentration exposure of human keratinocytes to endotoxin-free FLG or d-GO resulted in the secretion of specific pro-inflammatory cytokines (IL-1α, IL-6, IL-8, TNF-α, and GM-CSF) in the absence of cell death. However, despite these effects, the conditioned media collected from keratinocytes did not show any effect on the activation or migration of monocytes. It is noteworthy that the cytokine responses were seen after recovery (i.e., brief

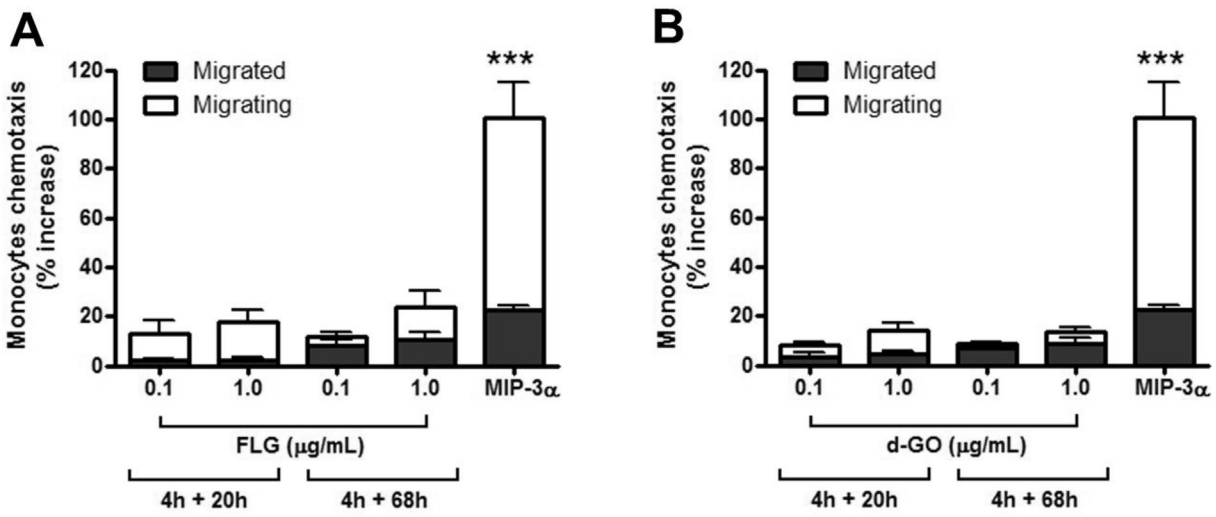

Fig. 8. No effect on THP-1 cell migration. HaCaT cells were exposed to FLG (A) or d-GO (B) under recovery conditions ("4h + 20h" and "4h + 68h") and subsequently co-cultured with THP-1 cells seeded in Transwell® inserts. After 4 h, migrated THP-1 cells were measured in the lower compartment, whereas migrating THP-1 cells were measured in the insert after repeated washes. Recombinant MIP-3α (1.25×10^{-12} M) was used as a positive control. Data are presented as % increase of chemotaxis of migrated and migrating cells in comparison to the untreated controls and are the mean values ± S.E. of 4 independent experiments. ***, $p < 0.001$ (One-way ANOVA and Bonferroni post-test).

exposure, followed by recovery in fresh medium), and not after continuous exposure, meaning that if only acute exposure is investigated then one would likely miss such effects. It is also noted that the cytokines tested are all known target genes of the transcription factor, NF-κB [45]. It is likely that the expression of pro-inflammatory cytokines is due to transcriptional upregulation of the corresponding genes, possibly in an NF-κB-dependent manner, and this may explain why the expression of cytokines in our model is more pronounced after recovery. Keratinocytes are positioned at the outermost layer of the body and poised to respond to harmful stimuli with the secretion of numerous cytokines, chemokines, and other factors [20]. However, barrier cells, such as epithelial cells, express significant amounts of IL-1α already at steady state, and IL-1α is biologically active both as a pro-form and as a cleaved protein, unlike IL-1β where only the cleaved form is a fully active pyrogen [20]. Therefore, it is also possible that preformed stores of IL-1α are released by keratinocytes exposed to GBMs. Damage to keratinocytes is known to cause the release of IL-1α. IL-1α, in turn, stimulates further release of IL-1α and the release of other cytokines, such as IL-8, IL-6, and GM-CSF, leading to the activation of an inflammatory response [46]. Concentrated airborne particles (CAPs), with a size range of 0.1–2.5 μm, were recently shown to trigger the production of IL-1α in HaCaT cells [47]. However, in the latter study, concentrations between 5 and 25 μg/mL were used, and cells exposed to these concentrations of CAPs were found to suffer a minor, albeit significant, decrease in cell viability. In contrast, in the present study, no discernible cell death was noted in HaCaT cells exposed to GBMs despite a significant induction of IL-1α secretion, which was most pronounced in the case of FLG. IL-6 is also a multifunctional cytokine involved in the regulation of immune responses and inflammation and, when the skin is damaged, IL-6 and IL-1α secreted from keratinocytes trigger the recruitment of inflammatory cells [20]. The secretion of IL-1α and IL-6 is of particular interest, as a recent study has suggested that the secretion of these cytokines by HaCaT cells can classify skin sensitizers from non-sensitizers [48]. It is important to note that FLG, but not d-GO, affected IL-6, and that FLG exerted a pronounced effect on IL-1α as well. Thus, low concentrations of FLG could act as a skin sensitizer. However, we did not see changes in differentiation markers in THP-1 cells indicative of a sensitization (discussed below).

We also noted that d-GO triggered the secretion of IL-8. IL-8 (CXCL8) is a potent chemoattractant. However, we did not observe any chemoattractant effects of the HaCaT cells on THP-1 cells. The reasons for the selective cytokine responses observed in HaCaT cells exposed to FLG *versus* d-GO are not well understood, but may be related to the way in which these materials are recognized by the cells. One possible explanation is that oxygen-containing functional groups – present in d-GO but not in FLG – may affect d-GO reactivity towards macromolecules, therefore altering its biological effects. We did not detect any TNF-α production in macrophages nor in keratinocytes in the case of d-GO, while FLG only triggered a minor upregulation of TNF-α in keratinocytes at the highest concentration. These findings do not rule out the involvement of TLRs, but they confirm that the materials studied were endotoxin-free. In a different study, we showed that GO was capable of eliciting cell signaling in primary human neutrophils *via* changes exerted on plasma membrane lipids [49]. Other investigators, using uric acid crystals, provided evidence for receptor-independent sensing of solid structures *via* membrane lipid alterations leading to immune cell activation [50]. Furthermore, using a set of GO materials comprising pristine, reduced and hydrated GO, Li et al. recently showed that the surface oxidation state plays an important role for the toxicity of GO in lung epithelial cells and macrophages [51]. The latter experiments were conducted at high concentrations (up to 200 μg/mL). Whether the low-concentration effects of FLG and GO documented in HaCaT cells occur *via* receptor-dependent or -independent mechanisms remains to be elucidated. We recently exploited the Raman signature of GBMs to detect these materials in HaCaT cells, attesting to the ability of keratinocytes to internalize GBMs [18]. In the present study, we verified cellular uptake of FLG and d-GO by HaCaT cells by using TEM. The uptake mechanism of d-GO and FLG was not investigated though other authors have inferred, on the basis of both experimental and theoretical studies, that FLG may enter cells (including keratinocytes) through direct membrane penetration [52]. These observations do not explain the distinct cytokine responses elicited by FLG and d-GO; indeed plasma membrane perturbation alone may not be sufficient and other (intra)cellular events may also play a role.

The levels of cytokine, chemokine and growth factor secretion

by THP-1 cells exposed to conditioned media of GBM-treated HaCaT cells were not statistically different from those observed in the negative control, suggesting a negligible effect. Consistent with these results, the phenotypic analysis revealed that, in general, none of the conditioned media collected from FLG- or d-GO-treated HaCaT cells induced significant changes in the expression of differentiation markers (CD14, CD54, CD86, HLA-DR and CD11b) in THP-1 cells. We only observed a slight increase in the expression of HLA-DR after 120 h exposure to the "4h + 68h" conditioned medium obtained at the highest FLG concentration (1.0 μg/mL). To further characterize potential inflammatory effects, we investigated the possibility that HaCaT cells could promote THP-1 cell chemotaxis. Indeed, FLG and d-GO induced the secretion of IL-8/CXCL8, and FLG and d-GO also induced the release of IL-1α and TNF-α that are known to further induce the release of chemokines [53]. However, in a co-culture experiment with FLG or d-GO treated HaCaT cells and THP-1 cells, we could not provide evidence for a significant THP-1 migration. The lack of THP-1 cell migration is in line with the unaltered expression of changes in differentiation markers following the exposure to conditioned media. Furthermore, a previous study has shown that an upregulated expression of the co-stimulatory molecules, CD54 and CD86, on THP-1 cells may be useful to predict the sensitization potential of chemicals [54]. Taken together, our results argue against a sensitization potential of the tested GBMs. In general, we may conclude that, despite the capability of FLG and d-GO to initiate an inflammatory response by activating keratinocytes, these materials do not modulate monocyte activation and migration. Our results therefore suggest that low-concentration exposure of skin cells to GBMs may not be detrimental, which is relevant for the application of GBMs in wearable devices. However, the present results were obtained in a simplified setting consisting of keratinocyte- and monocyte-derived cell lines, and the results do not rule out a possible involvement of other immune-competent cells, such as neutrophils [55], or Langerhans' cells, the antigen-presenting cells of the skin. The use of 3D models, more predictive of the possible dermal outcomes, would also be useful to support the present results.

5. Conclusions

In conclusion, we provided evidence that sub-cytotoxic concentrations of FLG and d-GO induced pro-inflammatory mediator release in HaCaT cells, suggesting that these materials are capable of activating keratinocytes. However, keratinocyte activation did not trigger an inflammatory reaction in monocyte-like cells, as conditioned media collected from exposed HaCaT cells were found to be ineffective in inducing activation and migration of THP-1 cells. These results do not exclude the possibility that GBMs could impact on other immune-competent cells, and further studies on the cross-talk between keratinocytes and immune cells are warranted. Nevertheless, our results suggest that FLG and d-GO elicit limited effects upon cutaneous exposure when applied at low doses and, therefore, that these materials may be explored for applications in which devices are in contact with the skin.

Declaration of competing interest

The authors declare that they have no known competing financial interests or personal relationships that could have appeared to influence the work reported in this paper.

CRediT authorship contribution statement

Laura Fusco: Investigation, Writing - original draft. **Marco Pelin:** Conceptualization, Investigation, Writing - original draft. **Sourav Mukherjee:** Investigation. **Sandeep Keshavan:** Investigation. **Silvio Sosa:** Investigation. **Cristina Martín:** Investigation. **Viviana González:** Investigation. **Ester Vázquez:** Supervision, Writing - original draft. **Maurizio Prato:** Supervision, Funding acquisition, Writing - review & editing. **Bengt Fadeel:** Conceptualization, Supervision, Funding acquisition, Writing - review & editing. **Aurelia Tubaro:** Conceptualization, Supervision, Funding acquisition, Writing - review & editing.

Acknowledgements

Supported by the European Commission through the Graphene Flagship (grant agreement no. 696656, and 785219) and by the Spanish Ministerio de Economía y Competitividad (CTQ2017-88158-R). The authors thank Graphenea (San Sebastián) for generously providing GO for these studies, and IRCCS Burlo Garofolo for support in cytokine measurements in the HaCaT cell model. We also thank Dr. Lars Haag, EM Core Facility at Karolinska Institutet, for expert assistance with TEM.

Appendix A. Supplementary data

Supplementary data to this article can be found online at https://doi.org/10.1016/j.carbon.2019.12.064.

References

[1] W. Choi, I. Lahiri, R. Seelaboyina, Y.S. Kang, Synthesis of graphene and its applications: a review, Crit. Rev. Solid State Mater. Sci. 35 (2010) 52–71.
[2] V. Singh, D. Joung, L. Zhai, S. Das, S. Khondaker, S. Seal, Graphene based materials: past, present and future, Prog. Mater. Sci. 56 (2011) 1178–1271.
[3] R.J. Young, I.A. Kinloch, L. Gong, K.S. Novoselov, The mechanics of graphene nanocomposites: a review, Compos. Sci. Technol. 72 (2012) 1459–1476.
[4] K. Yang, L. Feng, H. Hong, W. Cai, Z. Liu, Preparation and functionalization of graphene nanocomposites for biomedical applications, Nat. Protoc. 8 (2013) 2392–2403.
[5] K. Bhattacharya, S.P. Mukherjee, A. Gallud, S.C. Burkert, S. Bistarelli, S. Bellucci, et al., Biological interactions of carbon-based nanomaterials: from coronation to degradation, Nanomedicine 12 (2016) 333–351.
[6] G. Reina, J.M. González-Domínguez, A. Criado, E. Vázquez, A. Bianco, M. Prato, Promises, facts and challenges for graphene in biomedical applications, Chem. Soc. Rev. 46 (2017) 4400–4416.
[7] S.R. Shin, Y.C. Li, H.L. Jang, P. Khoshakhlagh, M. Akbari, A. Nasajpour, et al., Graphene-based materials for tissue engineering, Adv. Drug Deliv. Rev. 105 (2016) 255–274.
[8] C. Choi, Y. Lee, K.W. Cho, J.H. Koo, D.-H. Kim, Wearable and implantable soft bioelectronics using two-dimensional materials, Acc. Chem. Res. 52 (2019) 73–81.
[9] B. Fadeel, C. Bussy, S. Merino, E. Vazquez, E. Flahaut, F. Mouchet, et al., Safety assessment of graphene-based materials: focus on human health and the environment, ACS Nano 12 (2018) 10582–10620.
[10] M. Pelin, S. Sosa, M. Prato, A. Tubaro, Occupational exposure to graphene based nanomaterials: risk assessment, Nanoscale 10 (2018) 15894–15903.
[11] J. Russier, E. Treossi, A. Scarsi, F. Perrozzi, H. Dumortier, L. Ottaviano, et al., Evidencing the mask effect of graphene oxide: a comparative study on primary human and murine phagocytic cells, Nanoscale 5 (2013) 11234–11247.
[12] M. Orecchioni, D.A. Jasim, M. Pescatori, R. Manetti, C. Fozza, F. Sgarrella, et al., Molecular and genomic impact of large and small lateral dimension graphene oxide sheets on human immune cells from healthy donors, Adv. Healthc. Mater. 5 (2016) 276–287.
[13] M. Orecchioni, D. Bedognetti, L. Newman, C. Fuoco, F. Spada, W. Hendrickx, et al., Single-cell mass cytometry and transcriptome profiling reveal the impact of graphene on human immune cells, Nat. Commun. 8 (2017) 1109.
[14] S.P. Mukherjee, K. Kostarelos, B. Fadeel, Cytokine profiling of primary human macrophages exposed to endotoxin-free graphene oxide: size-independent NLRP3 inflammasome activation, Adv. Healthc. Mater. 7 (2018) 4.
[15] A. Sasidharan, L.S. Panchakarla, A.R. Sadanandan, A. Ashokan, P. Chandran, C.M. Girish, et al., Hemocompatibility and macrophage response of pristine and functionalized graphene, Small 8 (2012) 1251–1263.
[16] K.H. Liao, Y.S. Lin, C.W. Macosko, C.L. Haynes, Cytotoxicity of graphene oxide and graphene in human erythrocytes and skin fibroblasts, ACS Appl. Mater. Interfaces 3 (2011) 2607–2615.
[17] M. Pelin, L. Fusco, V. Leon, C. Martin, A. Criado, S. Sosa, et al., Differential cytotoxic effects of graphene and graphene oxide on skin keratinocytes, Sci. Rep. 7 (2017) 40572.
[18] M. Pelin, L. Fusco, C. Martin, S. Sosa, J. Frontinan-Rubio, J.M. Gonzalez-

Dominguez, et al., Graphene and graphene oxide induce ROS production in human HaCaT skin keratinocytes: the role of xanthine oxidase and NADH dehydrogenase, Nanoscale 10 (2018) 11820–11830.
[19] J. Frontiñán-Rubio, M.V. Gómez, C. Martín, J.M. González-Domínguez, M. Durán-Prado, E. Vázquez, Differential effects of graphene materials on the metabolism and function of human skin cells, Nanoscale 10 (2018) 11604–11615.
[20] F.O. Nestle, P. Di Meglio, J.Z. Qin, B.J. Nickoloff, Skin immune sentinels in health and disease, Nat. Rev. Immunol. 9 (2009) 679–691.
[21] P. Di Meglio, G.K. Perera, F.O. Nestle, The multitasking organ: recent insights into skin immune function, Immunity 35 (2011) 857–869.
[22] J.M. Gonzalez-Dominguez, V. Leon, M.I. Lucio, M. Prato, E. Vazquez, Production of ready-to-use few-layer graphene in aqueous suspensions, Nat. Protoc. 13 (2018) 495–506.
[23] V. León, J.M. González-Domínguez, J.L.G. Fierro, M. Prato, E. Vázquez, Production and stability of mechanochemically exfoliated graphene in water and culture media, Nanoscale 8 (2016) 14548–14555.
[24] S.P. Mukherjee, N. Lozano, M. Kucki, A.E. Del Rio-Castillo, L. Newman, E. Vázquez, K, et al., Detection of endotoxin contamination of graphene based materials using the TNF-α expression test and guidelines for endotoxin-free graphene oxide production, PLoS One 11 (2016), e0166816.
[25] A. Gallud, O. Bondarenko, N. Feliu, N. Kupferschmidt, R. Atluri, A. Garcia-Bennett, et al., Macrophage activation status determines the internalization of mesoporous silica particles: exploring the role of different pattern recognition receptors, Biomaterials 121 (2017) 28–40.
[26] M. Pelin, C. Florio, C. Ponti, M. Lucafò, D. Gibellini, A. Tubaro, et al., Pro-inflammatory effects of palytoxin: an *in vitro* study on human keratinocytes and inflammatory cells, Toxicol Res 5 (2016) 1172–1181.
[27] K. Bhattacharya, G. Kilic, P.M. Costa, B. Fadeel, Cytotoxicity screening and cytokine profiling of nineteen nanomaterials enables hazard ranking and grouping based on inflammogenic potential, Nanotoxicology 11 (2017) 809–826.
[28] A. Rodrigues, L. Newman, N. Lozano, S. Mukherjee, B. Fadeel, C. Bussy, K. Kostarelos, Blueprint for the synthesis and characterisation of thin graphene oxide with controlled lateral dimensions for biomedicine, 2D Mater. 5 (2018), 035020.
[29] U. Mogera, R. Dhanya, R. Pujar, C. Narayana, G.U. Kulkarni, Highly decoupled graphene multilayers: turbostraticity at its best, J. Phys. Chem. Lett. 6 (2015) 4437–4443.
[30] A.C. Ferrari, J.C. Meyer, V. Scardaci, C. Casiraghi, M. Lazzeri, F. Mauri, et al., Raman spectrum of graphene and graphene layers, Phys. Rev. Lett. 97 (2006) 187401.
[31] F. Torrisi, T. Hasan, W. Wu, Z. Sun, A. Lombardo, T.S. Kulmala, et al., Inkjet-printed graphene electronics, ACS Nano 6 (2012) 2992–3006.
[32] J.L. Figueiredo, M.F.R. Pereira, M.M.A. Freitas, J.J.M. Órfão, Modification of the surface chemistry of activated carbons, Carbon 37 (1999) 1379–1389.
[33] S. Stankovich, D.A. Dikin, R.D. Piner, K.A. Kohlhaas, A. Kleinhammes, Y. Jia, et al., Synthesis of graphene-based nanosheets *via* chemical reduction of exfoliated graphite oxide, Carbon 45 (2007) 1558–1565.
[34] W. Chen, L. Yan, Preparation of graphene by a low-temperature thermal reduction at atmosphere pressure, Nanoscale 2 (2010) 559–563.
[35] B.C. Palmer, S.J. Phelan-Dickenson, L. Delouise, Multi-walled carbon nanotube oxidation dependent keratinocyte cytotoxicity and skin inflammation, Part. Fibre Toxicol. 16 (2019) 3.
[36] S.P. Mukherjee, O. Bondarenko, P. Kohonen, F.T. Andon, T. Brzicova, I. Gessner, et al., Macrophage sensing of single-walled carbon nanotubes *via* Toll-like receptors, Sci. Rep. 8 (2018) 1115.
[37] M. Kang, J. Kim, B. Jang, Y. Chae, J.-H. Kim, J.-H. Ahn, Graphene-based three-dimensional capacitive touch sensor for wearable electronics, ACS Nano 11 (2017) 7950–7957.
[38] N. Karim, S. Afroj, S. Tan, P. He, A. Fernando, C. Carr, K.S. Novoselov, Scalable production of graphene-based wearable e-textiles, ACS Nano 11 (2017) 12266–12275.
[39] S. Lee, I. Jo, S. Kang, B. Jang, J. Moon, J.B. Park, et al., Smart contact lenses with graphene coating for electromagnetic interference shielding and dehydration protection, ACS Nano 11 (2017) 5318–5324.
[40] Y. Yoshioka, E. Kuroda, T. Hirai, Y. Tsutsumi, K.J. Ishii, Allergic responses induced by the immunomodulatory effects of nanomaterials upon skin exposure, Front. Immunol. 8 (2017) 169.
[41] G. Qu, S. Liu, S. Zhang, L. Wang, X. Wang, B. Sun, et al., Graphene oxide induces toll-like receptor 4 (TLR4)-dependent necrosis in macrophages, ACS Nano 7 (2013) 5732–5745.
[42] Y. Li, M. Fujita, D. Boraschi, Endotoxin contamination in nanomaterials leads to the misinterpretation of immuno safety results, Front. Immunol. 8 (2017) 472.
[43] M.H. Lahiani, K. Gokulan, K. Williams, M.V. Khodakovskaya, S. Khare, Graphene and carbon nanotubes activate different cell surface receptors on macrophages before and after deactivation of endotoxins, J. Appl. Toxicol. 37 (2017) 1305–1316.
[44] M.A. Vetten, C.S. Yah, T. Singh, M. Gulumian, Challenges facing sterilization and depyrogenation of nanoparticles: effects on structural stability and biomedical applications, Nanomedicine 10 (2014) 1391–1399.
[45] M. Pasparakis, I. Haase, F.O. Nestle, Mechanisms regulating skin immunity and inflammation, Nat. Rev. Immunol. 14 (2014) 289–301.
[46] N.C. Di Paolo, D.M. Shayakhmetov, Interleukin 1α and the inflammatory process, Nat. Immunol. 17 (2016) 906–913.
[47] A. Romani, C. Cervellati, X.M. Muresan, G. Belmonte, A. Pecorelli, F. Cervellati, et al., Keratinocytes oxidative damage mechanisms related to airbone particle matter exposure, Mech. Ageing Dev. 172 (2018) 86–95.
[48] D. Jung, J.H. Che, K.M. Lim, Y.J. Chun, Y. Heo, S.H. Seok, Discrimination of skin sensitizers from non-sensitizers by interleukin-1α and interleukin-6 production on cultured human keratinocytes, J. Appl. Toxicol. 36 (2016) 1129–1136.
[49] S.P. Mukherjee, B. Lazzaretto, K. Hultenby, L. Newman, A.F. Rodrigues, N. Lozano, et al., Graphene oxide elicits membrane lipid changes and neutrophil extracellular trap formation, Chem 4 (2018) 334–358.
[50] G. Ng, K. Sharma, S.M. Ward, M.D. Desrosiers, L.A. Stephens, W.M. Schoel, et al., Receptor-independent, direct membrane binding leads to cell-surface lipid sorting and Syk kinase activation in dendritic cells, Immunity 29 (2008) 807–818.
[51] R. Li, L.M. Guiney, C.H. Chang, N.D. Mansukhani, Z. Ji, X. Wang, et al., Surface oxidation of graphene oxide determines membrane damage, lipid peroxidation, and cytotoxicity in macrophages in a pulmonary toxicity model, ACS Nano 12 (2018) 1390–1402.
[52] Y. Li, H. Yuan, A. von dem Bussche, M. Creighton, R.H. Hurt, et al., Graphene microsheets enter cells through spontaneous membrane penetration at edge asperities and corner sites, Proc. Natl. Acad. Sci. U. S. A. 110 (2013) 12295–12300.
[53] M.D. Turner, B. Nedjai, T. Hurst, D.J. Pennington, Cytokines and chemokines: at the crossroads of cell signalling and inflammatory disease, Biochim. Biophys. Acta 1843 (2014) 2563–2582.
[54] Y. Yoshida, H. Sakaguchi, Y. Ito, M. Okuda, H. Suzuki, Evaluation of the skin sensitization potential of chemicals using expression of co-stimulatory molecules, CD54 and CD86, on the naive THP-1 cell line, Toxicol. In Vitro 17 (2003) 221–228.
[55] S. Keshavan, P. Calligari, L. Stella, L. Fusco, L.G. Delogu, B. Fadeel, Nano-bio interactions: a neutrophil-centric view, Cell Death Dis. 10 (2019) 569.